Biochemical Pharmacology 96 (2015) 39–51

Contents lists available at ScienceDirect

Biochemical Pharmacology

journal homepage: www.elsevier.com/locate/biochempharm

# GCDCA down-regulates gene expression by increasing Sp1 binding to the NOS-3 promoter in an oxidative stress dependent manner

Sandra González-Rubio [a], Laura López-Sánchez [a,b], Juan Muñoz-Castañeda [a], Clara I. Linares [a], Patricia Aguilar-Melero [a], Manuel Rodríguez-Perálvarez [a,c], Rafael Sánchez-Sánchez [d], Ana Fernández-Álvarez [e], Marta Casado [c,e], Jose L. Montero-Álvarez [a,c], Antonio Rodríguez-Ariza [a,b], Jordi Muntané [a,c,2], Manuel de la Mata [a,c,1,*], Gustavo Ferrín [a,c,1,*]

[a] Maimonides Institute of Biomedical Research (IMIBIC), Reina Sofía Hospital, University of Córdoba, Córdoba 14004, Spain
[b] Spanish Cancer Network (RTICC), Instituto de Salud Carlos III, Córdoba 14004, Spain
[c] Biomedical Research Centre Network, Digestive and Liver Diseases (CIBEREHD), Instituto de Salud Carlos III, Córdoba 14004, Spain
[d] Anatomical Pathology Service, Reina Sofia University Hospital, Córdoba 14004, Spain
[e] Biomedicine Institute of Valencia (IBV-CSIC), Valencia 46010, Spain

ARTICLE INFO

*Article history:*
Received 10 March 2015
Accepted 23 April 2015
Available online 27 April 2015

*Keywords:*
Cholestatic liver disease
Endothelial nitric oxide synthase
Oxidative stress
Transcription factor Sp1
Glycochenodeoxycholic acid

ABSTRACT

During the course of cholestatic liver diseases, the toxic effect of bile acids accumulation has been related to the decreased expression of endothelial nitric oxide synthase (NOS-3) and cellular oxidative stress increase. In the present study, we have investigated the relationship between these two biological events. In the human hepatocarcinoma cell line HepG2, cytotoxic response to GCDCA was characterized by the reduced activity of the respiratory complexes II + III, the increased expression and activation of the transcription factor Sp1, and a higher binding capacity of this at positions −1386, −632 and −104 of the NOS-3 promoter (pNOS-3). This was associated with a decreased promoter activity and a consequent reduction of NOS-3 expression. The use of antioxidants in GCDCA-treated cells caused a lower activation of Sp1 and the recovery of the pNOS-3 activity and NOS-3 expression and activity. Similarly, the specific inhibition of Sp1 resulted in the improvement of NOS-3 expression. Both, antioxidant treatment and Sp1 inhibition were associated with the reduction of cell death-related parameters. Bile duct ligation in rats confirmed *in vitro* results concerning the activation of Sp1 and the reduction of NOS-3 expression. Our results provide direct evidence for the involvement of Sp1 in the regulation of NOS-3 expression during cholestasis. Thus, the identification of Sp1 as a potential negative regulator of NOS-3 expression represents a new mechanism by which the accumulation of bile acids causes a cytotoxic effect through the oxidative stress increase, and provides a new potential target in cholestatic liver diseases.



*Abbreviations:* ADHP, 0-acetyl-3, 7-dihydroxyphenoxazine; ALT, alanine aminotransferase; AST, aspartate aminotransferase; BDL, bile duct ligation group; CLD, cholestatic liver disease; DHE, dihydroethidium; ERK1/2, extracellular-signal-regulated kinase; GAPDH, glyceraldehyde 3-phosphate dehydrogenase; GCDCA, Glycochenodeoxycholic acid; $GGT_Y$, -glutamyltranspeptidase; GPX, glutathione peroxidase; HDAC, histone deacetylase; $H_2$DCFDA, 2,7-dichlorodihydrofluorescein diacetate; $H_2O_2$, hydrogen peroxide; JNK, cJun-terminal kinase; LDH, lactate dehydrogenase; MAPK, mitogen-activated protein kinase; MitA, mithramycin A; MitoQ, mitochondria-targeted ubiquinone; MnTBAP, manganese (III) tetrakis (4-benzoic acid) porphyrin chloride; NO, nitric oxide; NOS, nitric oxide synthase; NOS-3, endothelial NOS; $O_2^{\bullet -}$, superoxide anion radical; OXPHOS, oxidative phosphorylation; pNOS-3, NOS-3 promoter; ROS, reactive oxygen species; SO, Sham operated control group; SOD, superoxide dismutase; TA, tolfenamic acid; TFBS, transcription factors binding sites.

* Corresponding author at: Maimonides Institute of Biomedical Research (IMIBIC), Reina Sofía Hospital, Avda. Menéndez Pidal s/n, 14004 Córdoba, Spain. Tel.: +34 957213808; fax: +34 957010452.
*E-mail address:* gusfesa@gmail.com (G. Ferrín).
[1] These two authors have contributed equally to the study.
[2] Present address: Department of General Surgery, Hospital Universitario Virgen del Rocío-Virgen Macarena/IBiS/CSIC/Universidad de Sevilla, Seville, Spain.

http://dx.doi.org/10.1016/j.bcp.2015.04.017
0006-2952/

## 1. Introduction

Bile salt synthesis, secretion and recycling represent crucial liver functions for the maintenance of metabolic homeostasis. During cholestatic liver disease (CLD), toxic bile acids are accumulated in serum and liver as a consequence of their impaired formation and excretion into the hepatocyte canaliculus, which can result in fibrosis, cirrhosis and chronic liver failure [1]. It has been proposed that the deleterious effect of the accumulation of bile acids during cholestasis is related to oxidative stress. Thus, liver injury occurring from the bile duct ligation has been associated with mitochondrial dysfunction, which is an important source of reactive oxygen species (ROS), and disturbances in the antioxidant system [2,3].

Nitric oxide (NO) is a well-known pleiotropic agent influencing multiple aspects of the liver physiopathology. Depending on factors such as its concentration or generating source, NO has been reported to act as a primary mediator of liver damage or as a potent protective against hepatic injury [4]. In liver, NO can be synthesized by the activity of the three known isoforms of nitric oxide synthase (NOS), the endothelial isoform (NOS-3) being considered as the main source of endogenous NO [5]. The use of molecular treatments associated with the increase of NOS-3 expression and activity in CLD has shown a beneficial effect for the liver [6,7]. In addition, the administration of antioxidants reduces the hepatotoxicity of bile acids *in vitro* [8–10] and *in vivo* [3], through the prevention of NOS-3 expression decrease and the detoxification of ROS [11]. Thus, bioreactivity of NO mitigates the effect of ROS production [12]. Besides its role in ROS detoxification, NO can act as a cytoprotective agent by inhibiting caspases through direct nitrosylation [13].

Glycochenodeoxycholic acid (GCDCA) is a bile salt generated in the liver from chenodeoxycholic acid and glycine, whose relatively high toxicity and concentration in bile and serum after cholestasis has extended its use in cellular models of the disease [8–10]. Previously, we have reported that NOS-3 expression is decreased in the human hepatocarcinoma cell line HepG2 in response to GCDCA, and that the recovery of its expression and activity is related to the cytoprotective action of antioxidant molecules [8,9]. In the present study we set out to identify the elements responsible for regulating NOS-3 expression during CLD, as well as to analyse the role of oxidative stress in this process. Clarifying molecular mechanisms underlying hepatocellular cytotoxicity related to cholestasis disorders could be helpful for the design and development of new interventional strategies and treatments.

## 2. Materials and methods

### 2.1. Cell lines and culture conditions

The human hepatocarcinoma cell line HepG2 (European Collection of Cell Cultures) was routinely maintained as previously reported [8,9]. The pGL4-NOS3 cell line was obtained by stable transfection of HepG2 cells with the plasmid pGL4.20 [luc2/Puro] (Promega, Wisconsin, USA) containing the luciferase reporter gene under the control of the human NOS-3 promoter (pNOS-3; 1601 nucleotides, GenBank accession no. AF387340.1; Fig. 1). Dr. Huige Li (Department of Pharmacology, Johannes Gutenberg

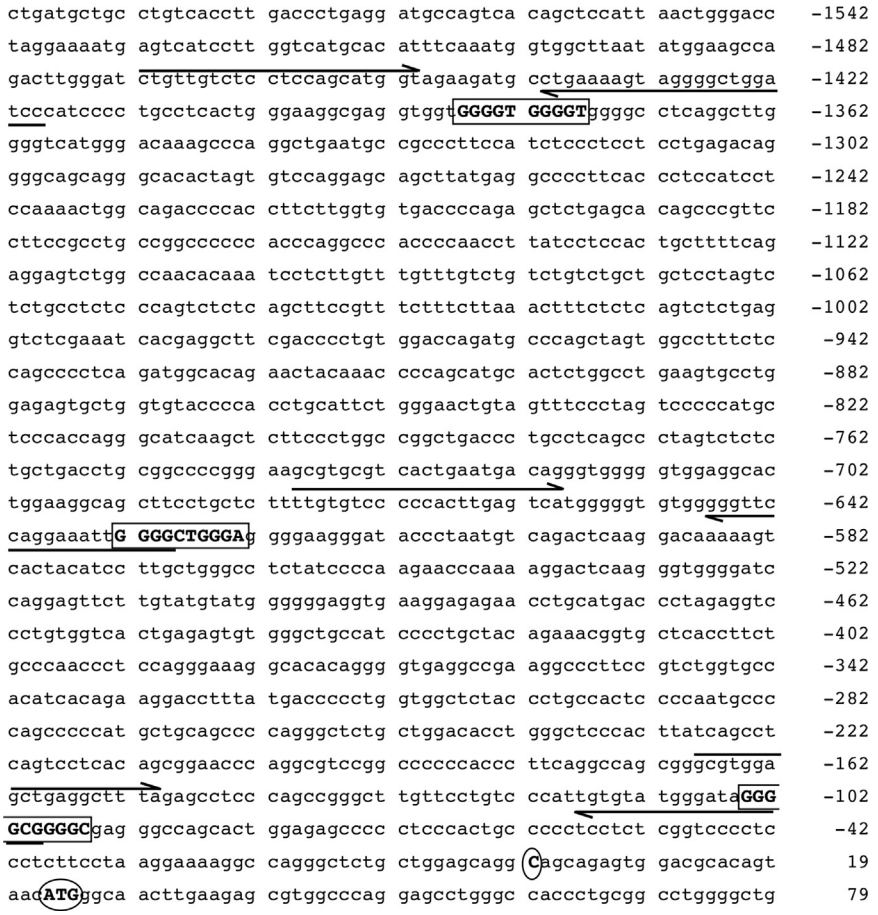


**Fig. 1.** Nucleotide sequence of the human NOS-3 promoter. Sequence of 1601 bases of the 5′-flanking region of the human NOS-3 gene (GenBank accession number AF387340.1). Circles: start codon ATG, and position −1 of the pNOS-3; Boxes: Sp1 Binding Sites; Arrows: Forward/Reverse primers used in ChIP assays.

University, Mainz, Germany) kindly donated the pNOS-3 sequence and no sequence variations were detected after vector construction. The control cell line pGL4 was obtained by stable transfection of HepG2 cells with the pGL4.20 [luc2/Puro] vector, without promoter sequence insertion. For the establishment of the cell lines, 75,000 cells/cm$^2$ were transfected with the appropriate vector, using the Fugene6 transfection reagent (Roche, Basel, Switzerland) in 1:3.5 ratio (μg plasmid DNA:μl Fugene6). Transfected cells were selected by adding 2 μg/ml puromycin (Sigma-Aldrich, Missouri, USA) to the culture medium. Thirteen cell clones for pGL4-NOS3 were isolated after antibiotic selection.

### 2.2. In vitro *studies*

#### 2.2.1. *Experimental procedure*

Cells were plated at 150,000 cells/cm$^2$ and 0.5 mM GCDCA (Sigma-Aldrich) was administered after 48 h of cell culture. The SOD mimetic MnTBAP (manganese (III) tetrakis (4-benzoic acid) porphyrin chloride) (Calbiochem, Darmstadt, Germany) and the mitochondria-targeted antioxidant MitoQ were administered at concentration of 0.1 mg/ml and 1 μM, respectively. Specific Specificity protein (Sp) transcription factor (TF) inhibitors tolfenamic acid (TA) and mithramycin A (MitA) were used at 60 μM and 20 nM, respectively (Sigma-Aldrich). Cells were harvested at different times according to the parameter under study. MitoQ was synthesized according to the procedure described by Kelso et al. [14].

### 2.3. In vivo *studies*

#### 2.3.1. *Experimental animal model of cholestasis*

Male Wistar rats (200–250 g) were kept in controlled conditions of light and temperature, and were provided with food and water *ad libitum* before and after surgery. Animals were treated according to institutional guidelines, and approval to conduct this study was granted by the Reina Sofía University Hospital Research Ethics Committee. Animals were randomized into two groups: Sham operated control group (SO group, $n = 13$) and bile duct ligation group (BDL group, $n = 13$). Surgical procedure and sample collection were carried out as we described before [15]. Briefly, 13 animals in each group were killed 7 days after surgery under sevofluorane anaesthesia. Blood was collected from the abdominal aorta and the serum obtained was frozen at −20 °C until the measurement of biochemical parameters. After perfusion with cold saline solution, the liver was rapidly removed for histological examination. Some liver specimens were frozen in liquid nitrogen and immediately stored at −80 °C for the subsequent analysis. Fig. 2 shows a representative scheme about the experimental procedure. It should be noted that in the BDL group there was death from the fifth day after surgery. On the seventh day of cholestasis (last day) the death rate was 35%. Only animals that survived biliary obstruction were considered in the BDL group.

### 2.4. *Preparation of cell extracts and tissue lysates*

Protein extracts from HepG2 were obtained by incubating the cells in a lysis buffer containing 50 mM Hepes, pH 7.5, 100 mM NaCl, 2 mM EDTA, 1% NP-40, 1 mM PMSF, 5 μg/ml aprotinin and 10 μg/ml leupeptin (Sigma-Aldrich). Rat liver lysates were obtained by mechanical disruption of liver tissue, using the Sample Grinding Kit (GE Healthcare, Buckinghamshire, UK) and the same buffer described above. The integrity and concentration of protein samples were determined by the Ponceau staining and the Bradford method, respectively.

### 2.5. *Evaluation of parameters of oxidative stress*

General ROS production and redox status was quantified by using the fluorescent probes dihydroethidium (DHE), 2,7-dichlorodihydrofluorescein diacetate ($H_2$DCFDA) and 10-acetyl-3, 7-dihydroxyphenoxazine (ADHP) (Life Technologies, California, USA). DHE detects cytosolic superoxide anion radical ($O_2^{\bullet -}$) and hydroxyl radical, and reacts with peroxynitrite-derived oxidants. $H_2$DCFDA detects hydrogen peroxide ($H_2O_2$) but also hydroxyl radical, carbonate radical, nitrogen dioxide and thiyl radicals resulting from thiol oxidation. ADHP oxidation is observed in the presence of $O_2^{\bullet -}$ and $H_2O_2$ [16]. Cells were incubated with 10 μM DHE or $H_2$DCFDA for 20 min and 30 min, respectively. After that, cells were washed with PBS and oxidative stress production was assessed *in situ* as the fluorescence emitted by DHE ($\lambda_{ex}$ = 510 nm/$\lambda_{em}$ = 590 nm) and $H_2$DCFDA ($\lambda_{ex}$ = 500 nm/$\lambda_{em}$ = 520 nm). Negative controls were carried out incubating cells with the corresponding treatment and without probe. The ADHP-based ROS detection kit was used following the manufacturer instruction. Briefly, HepG2 cells were collected and sonicated in PBS using a Bioruptor System UCD-200 (Diagenode, Liege, Belgium). After removing cell debris by centrifugation, the supernatants were aliquoted and stored at −80 °C until used. In the measurement, 50 μl from each sample were mixed 1:1 with the reaction mixture containing the 100 μM ADHP and 0.2 U/ml horseradish peroxidase, and the fluorescence increase over time was recorded using excitation at 550 nm and fluorescence detection at 595 nm.

### 2.6. *Enzymatic activity measurement of the respiratory complexes*

Mitochondria were isolated from cultured cells as previously described [17] and were used to measure the different enzymatic activities. Activities of citrate synthase (CS) and respiratory

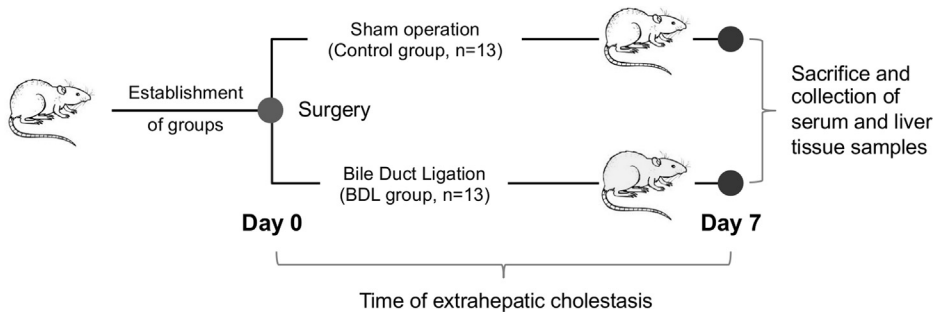


**Fig. 2.** Experimental design of the *in vivo* study. Before surgery, the animals were divided into two groups: sham operation group (control group, $n = 13$) and bile duct ligation group (BDL group, $n = 13$). A total of 7 days after the surgical procedure, animals from both groups were sacrificed by exsanguination and serum and liver tissue samples were properly collected and stored at −80° C until used.

complexes I, II, I + II, II + III and IV were measured by spectrophotometry as described in Lapuente-Brun et al. [18].

### 2.7. Cell death analysis

The apoptosis induction was assessed by the measure of caspase-3 activity in cell extracts and in rat liver lysates (100 μg of protein) as previously described [8,9]. Hepatocellular necrosis was evaluated through the cellular release of lactate dehydrogenase (LDH) as we previously described in [8]. The LDH release was calculated as the ratio of [((LDH culture medium)/(LDH cytoplasm + LDH culture medium)) × 100].

### 2.8. Evaluation of liver injury in bile duct ligated rats

Serum concentrations of Y-glutamyltranspeptidase (GGT), aspartate aminotransferase (AST), alanine aminotransferase (ALT) and total and direct bilirubin were determined by commercial assays as liver injury markers (Linear Chemicals SL, Barcelona, Spain).

### 2.9. NOS-3 promoter activity (luciferase reporter assay)

pGL4-NOS3 and pGL4 cells (15,000/well) were plated in 384-well black microplates. Luciferase activity was measured using the One-Glow Luciferase Assay System (Promega). Briefly, cells were lysed with 20 μl of 1× Lysis Buffer, and 40 μl of cell extract were used for luciferase assay according to the manufacturer's recommendations.

### 2.10. Gene expression analysis

Gene expression at the mRNA level was determined by quantitative real-time PCR using a One-Step QuantiTect SYBR-Green Kit (Qiagen, Limburg, Netherlands). Total cellular RNA was extracted, treated with RNAse-Free DNase and used as template for mRNA amplification with specific primers. Human primers (forward, F, and reverse, R) were located in the coding DNA sequence at positions described below: NOS-3 (NM_000603.4), F: 3697–3719, R: 3895–3873; glutathione peroxidase 4 (GPX4; NM_002085.3), F: 403–422, R: 609–587; catalase (NM_001752.3), F: 1028–1053, R: 1179–1159; superoxide dismutase 1 (SOD1; NM_000454.4), F: 430–451, R: 539–519; SOD2 (NM_001024465.1), F: 708–728, R: 867–845; ribosomal protein L13A (RPL13A; NM_012423.3), F: 541–563, R: 666–642. Rat primers were located at positions: Nos-3 (XM_006235872.1), F: 3274–3293, R: 3375-3355; Gpx1 (NM_030826.3), F: 312–332, R: 450–433; Gpx4 (NM_001039849.2), F: 542–561, R: 707–688; catalase (NM_012520.2), F: 1631–1654, R: 1706–1686; Sod1 (NM_017050.1), F: 219–237, R: 319–299; Sod2 (NM_017051.2), F: 226–245, R: 416–397; hypoxanthine phosphoribosyltransferase 1 (Hrpt1; NM_012583.2), F: 179–203, R: 301–277.

### 2.11. Protein expression analysis by Western blot

Between 80 and 100 μg of protein from cell extracts or rat liver lysates were separated in a 10–12% SDS-PAGE, transferred to nitrocellulose membrane and sequentially blotted against monoclonal or polyclonal primary antibodies. Primary antibodies were anti-NOS-3 (sc-654, dilution 1:200), anti-Sp1 (ref. sc-420/X, dilution 1:2000), anti-p-Sp1 (ref. ab37707, diluted 1:1000), anti-p-JNK (ref. sc-6254, diluted 1:300), anti-p-ERK1/2 (ref. 4370, diluted 1:2000) and β-Actin (ref. sc-47778, diluted 1: 10,000). All antibodies were from Santa Cruz Biotechnology (California, USA), except anti-p-Sp1 (Abcam, Cambridge, UK) and anti-p-ERK1/2 (Cell Signalling Technology, Massachusetts, USA). The densitometry analysis was performed by Quantity One software (v.4.4.0) (Bio-Rad, California, USA). β-Actin was used as a loading control in the analysis of protein expression that was performed in the HepG2 cell line. In the rat liver lysates, the results of the Sp1 expression analysis were represented as the phosphorylated/non-phosphorylated protein ratio. Similarly, NOS-3 protein expression in rat liver lysates was referred to the protein load (Ponceau staining). In this case, to avoid errors in the quantification of the NOS-3 expression as a result of using different gels for the analysis of numerous samples, we used one of the control samples as an internal standard in each of the gels. Thus, all samples in both groups control and BDL were referred to this unique sample.

### 2.12. Nitric oxide production

NO production was determined by the Griess reaction as we previously described [9]. In order to allow the accumulation of NO-related end products nitrates and nitrites, the cell culture medium was collected 24 h after the administration of the treatment. This ensured the sensitivity and reproducibility of the reaction. Nitrite concentrations were accurately determined by a nitrite calibration curve.

### 2.13. Identification of transcription factors binding sites in the pNOS-3

The identification of theoretical transcription factors binding sites (TFBS) in the pNOS-3 sequence was performed using the three different free online software tools for TFBS prediction: Transcription Factor Search (TFsearch v.1.3; http://www.cbrc.jp.reserach/db/TFSEARCH.html), Transcription Element Search System (TESS; http://www.cbil.upenn.edu/tess) and Transcription Factor Site Scan (TF site scan; http://www.ifti.org/cgi-bin/ifti/Tfsitescan.pl).

### 2.14. Chromatin immunoprecipitation (ChIP)–RT-qPCR assay

ChIP-assays were performed as we previously described [19], using isolated nuclei from the formaldehyde-cross-linked HepG2 cells. Immunoprecipitation was performed using primary antibody anti-Sp1 and magnetic beads (Dynabeads® Protein G, Life Technologies). RNA polymerase II (PolII) and normal rabbit IgG were used as positive and negative control, respectively, using antibodies anti-PolII (ref. sc-899) and anti-IgG (ref. sc-2027). 4 μg of antibody was used for each experiment. All primary antibodies were from Santa Cruz Biotechnology. Purified samples were analysed by RT-qPCR, using SensiFast SYBR kit (Bioline, London, UK) and primers used to detect target sequences were as follows (Fig. 1): -1386 Sp1 site, 5′-CTGTTGTCTCCTCCAGCATGGT-3′ and 5′-GGATCCAGCCCCTACTTTTCAG-3′; -632 Sp1 site, 5′-TTGTGTCCCCCACTTGAGTCA-3′ and 5′-CCCCAATTTCCTGGAACCC-3′; -104 Sp1 site, 5′-GCGTGGAGCTGAGGCTTTA-3′ and 5′-CGCCCCTATCCCATACACA-3′; NOS-3 coding region (NM_000603.4), 5′-CCGGGACTTCATCAACCAGTA-3′ (positions 677–697 in exon 4) and 5′-TCCGGGAAGCTGTCACCTC-3′ (position exon 4/intron 4–5); glyceraldehyde 3-phosphate dehydrogenase (GAPDH) coding region (NM_002046.4), 5′-AGCCACATCGCTCAGACACC-3′ (position 155–174 in exon 2) and 5′-ACCCGTTGACTCCGACCTT-3′ (position exon 2/intron 2–3). For quantification purposes, a calibration curve was elaborated for each amplicon by 10-fold serial dilutions of the total input sample. Results were expressed as percent of input considering the input as 100% and the negative control as 0%.

### 2.15. Immunohistochemical analysis

The expression of CD68 was analysed by immunohistochemistry in 4% paraformaldehyde-fixed paraffin-embedded liver tissue sections (4 μm) mounted on glass slides coated with poly-L-lysine. The sections were dewaxed in xylene, rehydrated in ethanol and

incubated at 100 °C in ChemMate Target Retrieval Solution, pH 6.0 (Dako, Barcelona, Spain) for 20 min. After washing in PBS, the sections were immunostained using an autostainer (Cytomation, Dako). Slides were incubated for 10 min in 3% $H_2O_2$ to block endogenous peroxidase and then incubated for 1 h with anti-CD68 antibody (Santa Cruz Biotechnology; ref. sc-59103; 1:50 dilution). After washing 5 min in PBS, the slides were incubated for 30 min with an HRP-labelled polymer (Envision System, Dako) and developed for 15 min using diaminobenzidine. Finally, the slides were counterstained with hematoxylin and mounted in Eukitt mounting medium (Sigma-Aldrich).

### 2.16. Statistical analysis

Results were expressed as mean ± standard error of a minimum of 3 independent experiments. Data were compared using the non-parametric method Kruskal-Wallis, and the Dunnett's T3 test as post hoc multiple comparison analysis. Data from ChIP analysis and respiratory activity experiments, involving control and GCDCA-treated samples, as well as those from the *in vivo* study were analysed with the Mann-Whitney *U* test. Statistical differences were set at $p < 0.05$ in all studies. All tests and calculations were done with the statistical package StatView 5.0 (SAS Institute, Inc.) and SPSS 15.0 (IBM) for Windows.

## 3. Results

### 3.1. GCDCA induces cell death associated with oxidative stress increase and antioxidant system dysfunction

In HepG2 cells, the administration of GCDCA induced oxidative stress (268% for DHE, $p = 0.045$; 386% for $H_2$DCFDA, $p = 0.002$; 219% for ADHP, $p = 0.049$) (Fig. 3A) and cell death (222% for caspase-3 activity, $p = 0.002$; 186% for LDH release, $p = 0.006$) (Fig. 3B and C). This coincided with a decrease in the activity of the oxidative phosphorylation (OXPHOS) system (Fig. 4A) and with disturbances in the cellular antioxidant system (Fig. 4B). Thus, GCDCA caused the inhibition of the respiratory complex II + III activity (56%, $p < 0.001$) and the expression deregulation of the antioxidant genes SOD1 (55%, $p = 0.002$), SOD2 (42%, $p < 0.001$) and catalase

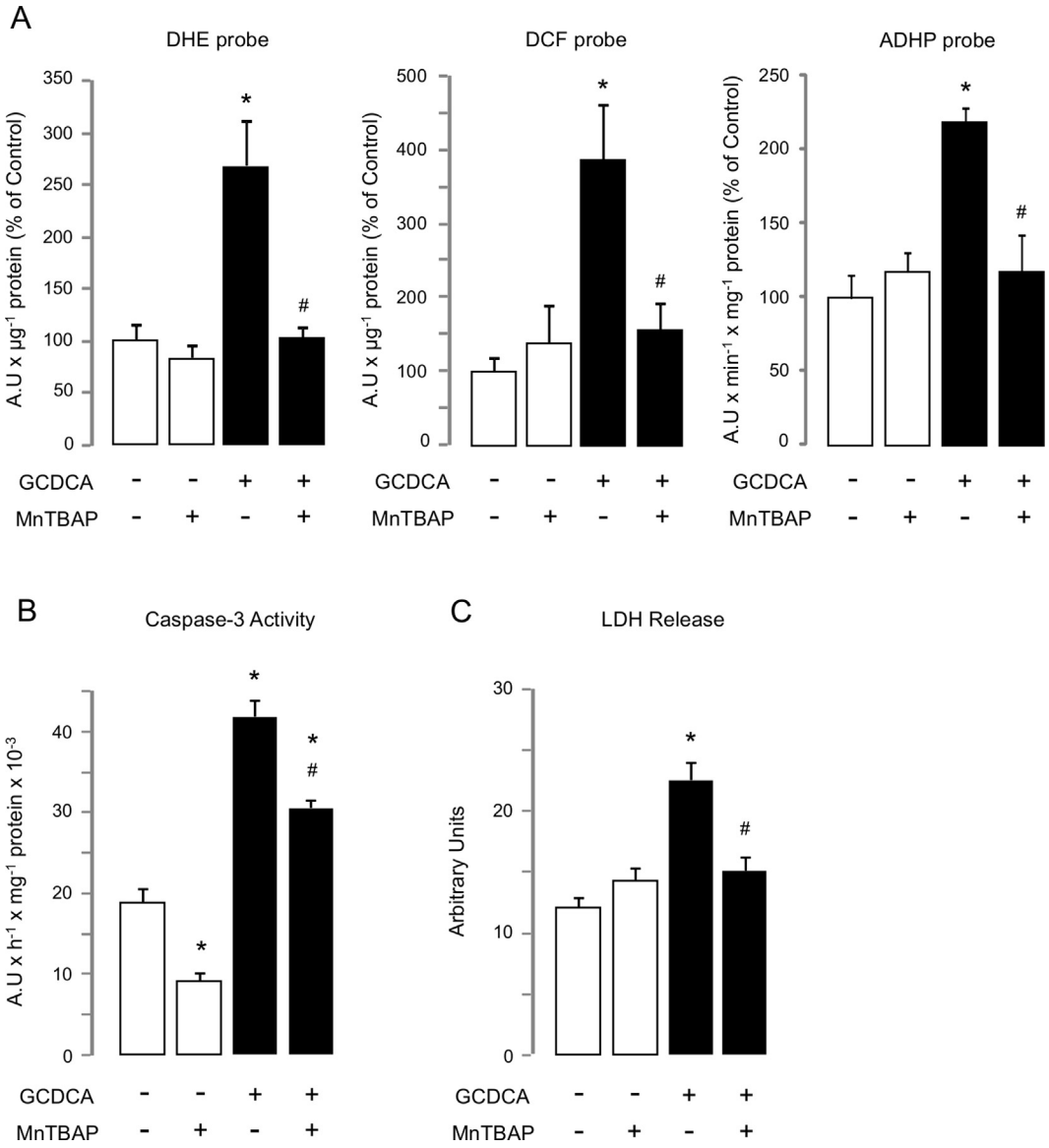


**Fig. 3.** GCDCA induces oxidative stress and cell death in HepG2 cells. (A) Overall ROS production was quantified by using the fluorescent probes DHE, $H_2$DCFDA and ADHP ($n = 3$). Cell death was assessed by the measure of (B) caspase-3 activity ($n = 5$) and (C) LDH release ($n = 4$). The parameters were determined at 6 h (A) or 24 h (B and C) after GCDCA and/or MnTBAP administration. Data expressed as mean ± SE. Statistically significant difference versus control group* or versus GCDCA group# are marked.

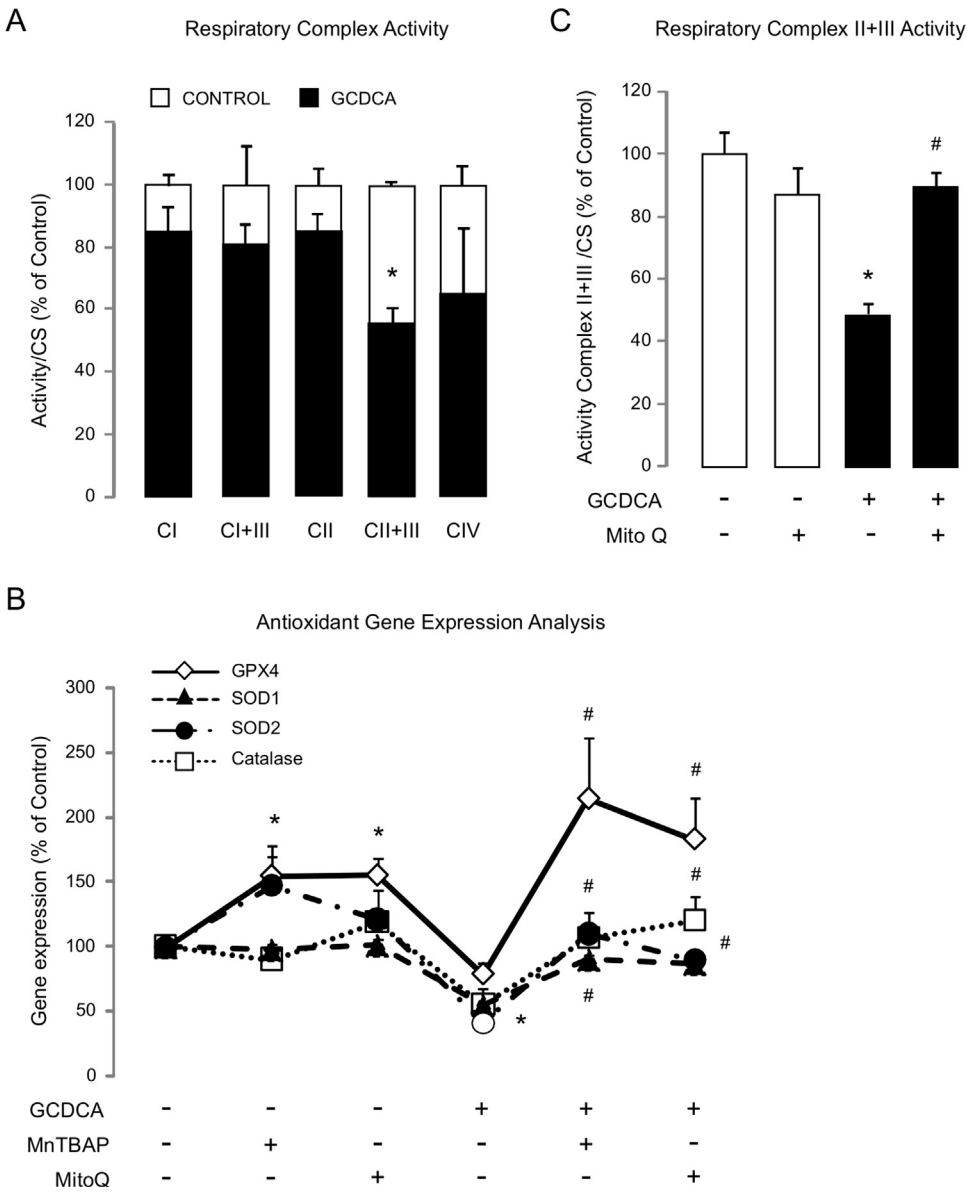


**Fig. 4.** Deregulation of respiratory activity and the antioxidant gene expression in GCDCA-treated cells. (A) Activity of respiratory complexes I, I + III, II, II + III and IV ($n = 6$). Citrate synthase (CS) activity was used as a normalizing. (B) Quantification of gene expression by RT-qPCR ($n = 6$). (C) Activity of respiratory complex II + III ($n = 6$). Cells not exposed/exposed to GCDCA were treated with MnTBAP or MitoQ. The parameters were determined at 6 h after GCDCA and/or MnTBAP or MitoQ administration. Data expressed as mean ± SE. Statistically significant difference versus control group* or versus GCDCA group# are marked.

(55%, $p < 0.001$). The administration of MnTBAP reduced the hepatocellular damage (Fig. 3B and C) by preventing ROS production (Fig. 3A) and by modulating the antioxidant defense machinery (Fig. 4B) in GCDCA-treated HepG2 cells. Thus, MnTBAP recovered the gene expression level of SOD1, SOD2, GPX4 and catalase. Likewise, in the presence of the bile salt, MitoQ restored the activity of the respiratory complex II + III (Fig. 4C) and the basal expression of antioxidant genes (Fig. 4B).

### 3.2. Oxidative stress induced by GCDCA negatively regulates the transcriptional activity of pNOS-3 and NOS-3 expression and activity

As Fig. 5 shows, GCDCA administration decreased: (A) transcriptional activity of pNOS-3 (46%, $p = 0.021$), (B) NOS-3 mRNA levels (41%, $p = 0.015$), (C) NOS-3 protein expression (64%, $p = 0.046$) and (D) the end products of NO oxidation, nitrites and nitrates (64%, $p = 0.021$). MnTBAP treatment reversed the described effects associated with the administration of the bile acid, and totally/partially recovered the pNOS-3 activity, NOS-3 mRNA and protein levels and nitrite/nitrate production. Similarly, the administration of the mitochondria-targeted antioxidant MitoQ recovered the pNOS-3 activity (Fig. 5A).

### 3.3. GCDCA-induced oxidative stress stimulates the expression and activation of Sp1

Bioinformatic analysis of the pNOS-3 sequence identified three candidate binding sites for Sp1, which could be involved in the modulation of NOS-3 expression. These Sp1 binding sites were identified unanimously by the three prediction programs used at positions described in Table 1. To elucidate whether Sp1 was involved in the NOS-3 regulation during cytotoxicity by GCDCA, we determined its expression and activation rates in HepG2 cells. GCDCA increased the protein expression level (166%, $p = 0.008$)

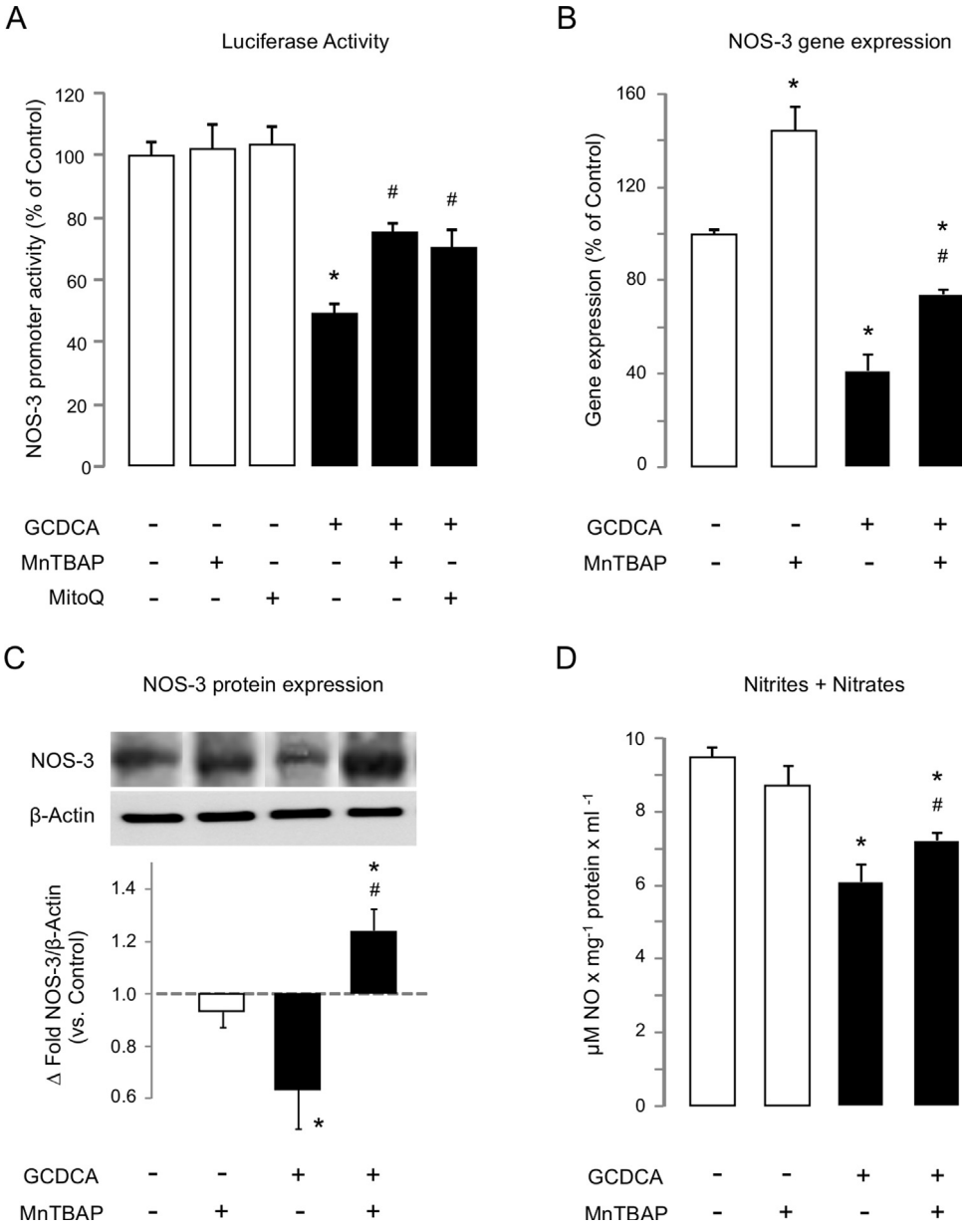


**Fig. 5.** Effect of GCDCA-induced oxidative stress on NOS-3 expression and activity. (A) NOS-3 promoter activity ($n = 4$). (B) NOS-3 gene expression ($n = 4$). (C) NOS-3 protein expression ($n = 3$). (D) NO-related end products ($n = 3$). The parameters were determined at 6 h (A), 12 h (B) and 24 h (C and D) after GCDCA and/or MnTBAP administration. Data expressed as mean ± SE. Statistically significant difference versus control group* or versus GCDCA group# are marked.

and phosphorylation state (200%, $p = 0.003$) of Sp1. Because the expression and activation of Sp1 can be regulated by the mitogen-activated protein kinase (MAPK) pathway, we next analysed the activation state of kinases JNK (cJun-terminal kinase) and ERK1/2 (extracellular-signal-regulated kinase). GCDCA administration increased the protein levels of phospho-JNK (235%, $p < 0.001$) and phospho-ERK1/2 (389% $p = 0.015$/271% $p = 0.034$) in HepG2 cells. Cellular protection against oxidative injury by treatment with any of the described antioxidants, MnTBAP or MitoQ, reduced the expression and phosphorylation rates of Sp1 and the activation of MAPKs JNK and ERK1/2 during GCDCA-induced cytotoxicity (Fig. 6A and B).

**Table 1**
Proposed Sp1 binding sites in the NOS-3 promoter region (1.6 kb, GenBank accession no. AF387340.1).

| TF | TFSEARCH | | TESS | | TFSITESCAN | |
|---|---|---|---|---|---|---|
| | Position | Sequence | Position | Sequence | Position | Sequence |
| Sp1 | −1386 | GGGGTGGGGT | −1384 | GGTGGG | −1385 | CCCACC |
| | −632 | GGGGCTGGGA | −632 | KRGGCKRRK | −632 | KRGGCKRRK |
| | −104 | GGGGCGGGGC | −104 | GGGGCGGGGC | −104 | GGGGCGGGGC |

K is G/T, R is A/G.

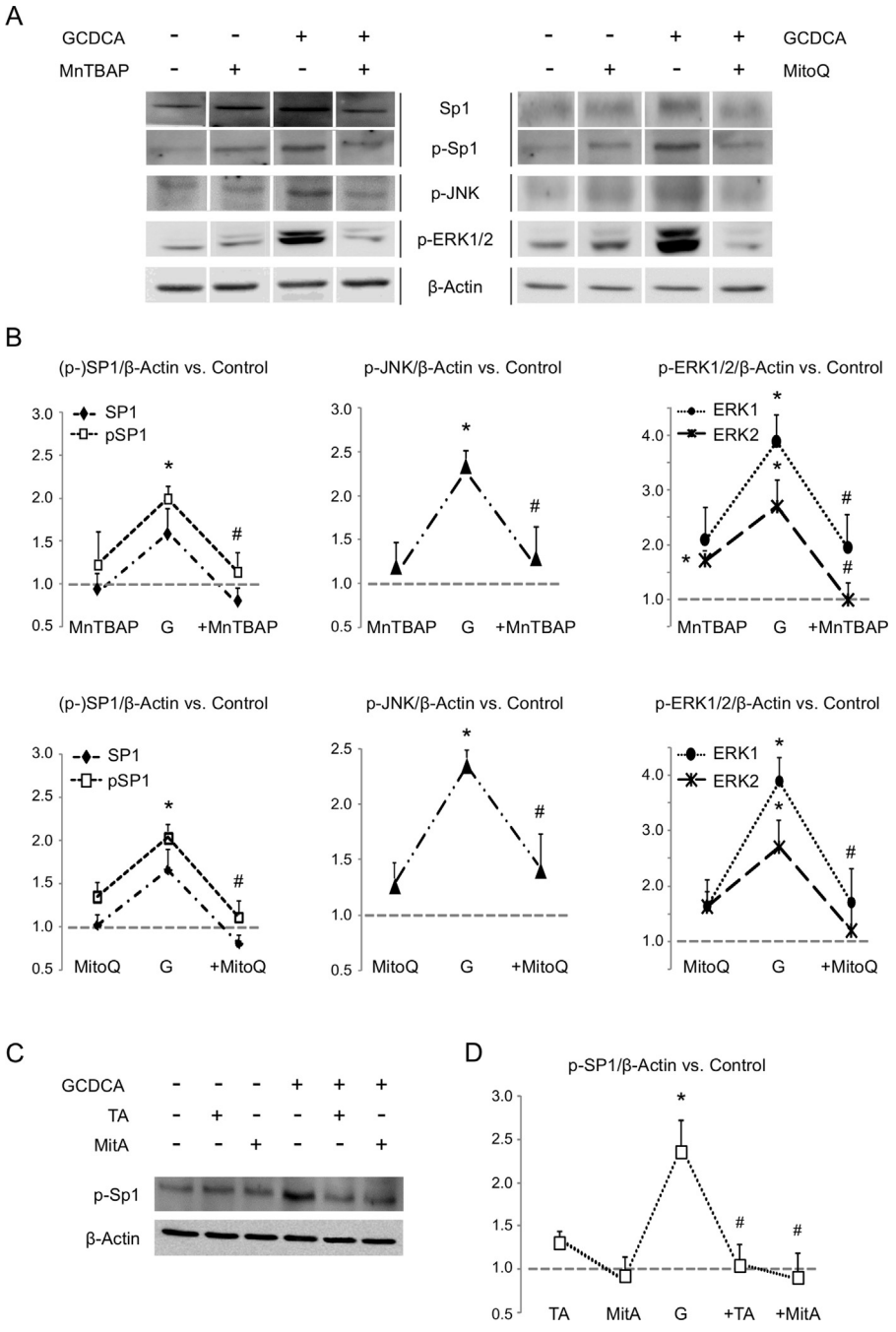


**Fig. 6.** Expression of Sp1 and MAPKs in GCDCA-treated cells. (A) Effect of the administration of MnTBAP or MitoQ (12 h). Representative western blots for (p-)Sp1 ($n$ = 4 and 5, respectively), p-JNK ($n$ = 3) and p-ERK1/2 ($n$ = 3) in HepG2 cell lysates. (B) Densitometry analysis of blots included in panel A. (C) Effect of the administration of Sp1 inhibitors, Tolfenamic acid (TA) and Mithramycin A (MitA) (6 h). Representative western blot for p-Sp1 ($n$ = 3) in cell lysates. (D) Densitometry analysis of blots included in panel C. In the densitometry analysis, the "+" sign indicates GCDCA-G- administration plus the showed treatment. Data as mean ± SE. Statistically significant difference versus control group* or versus GCDCA group# are marked.

### 3.4. Sp1 participates in NOS-3 downregulation during GCDCA-induced cytotoxicity

Then, we evaluated the involvement of Sp1 in the NOS-3 regulation during GCDCA-induced cell death by testing specific inhibitors TA and MitA. Fig. 6C and D shows the effect of TF inhibitors on the phosphorylation state of Sp1. Both of inhibitors were able to inhibit the GCDCA-induced activation of Sp1.

When we later investigated the effect of Sp1 inhibition in GCDCA-treated pGL4-NOS3 cells, we found that both TA and MitA were able to restore the pNOS-3 transcriptional activity (Fig. 7A) and the NOS-3 protein expression (Fig. 7B). This fact was related to a higher extracellular concentration of NO-oxidation end products (Fig. 7C) and to a marked reduction on caspase-3 activity (Fig. 7D). No additional effect on pNOS-3 activity was observed when Sp1 inhibitors were combined (data not shown).

### 3.5. GCDCA increases Sp1 binding to pNOS-3

In order to test the effect of GCDCA administration on the Sp1 binding capacity to the pNOS-3 sequence, we performed ChIP assay. We selected the three candidates Sp1 binding sites

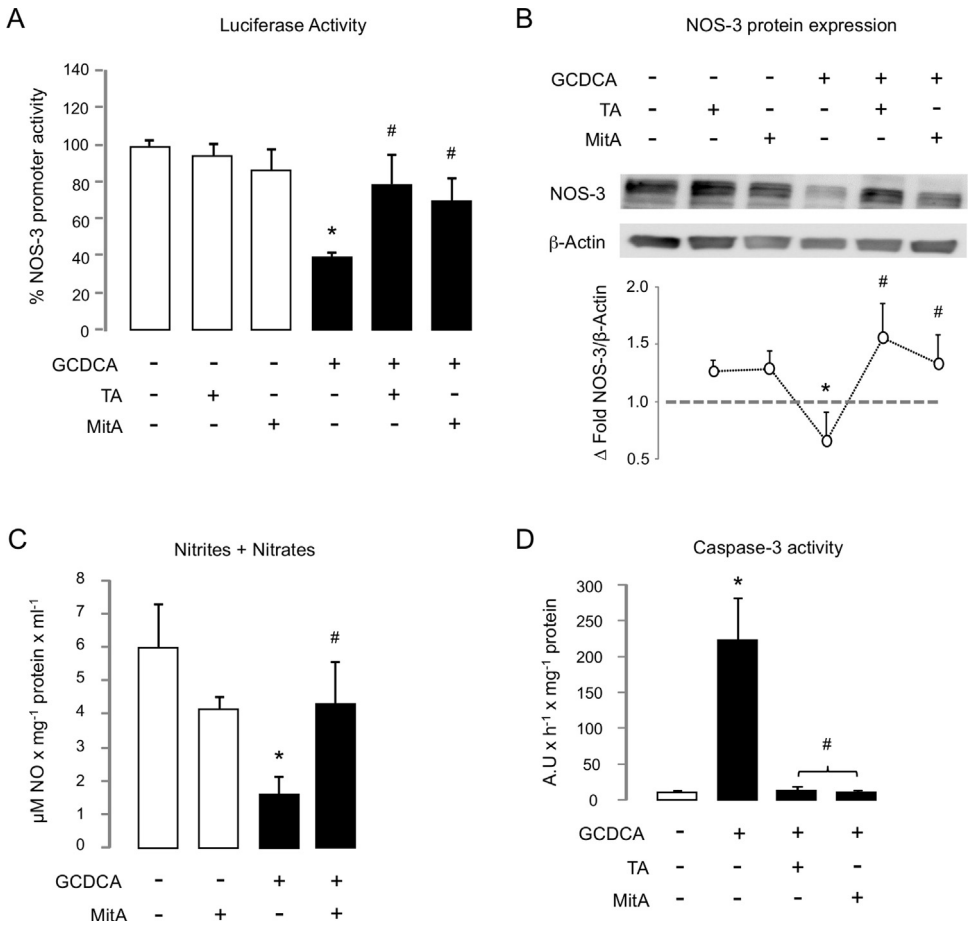


**Fig. 7.** Role of Sp1 in NOS-3 regulation during cytotoxicity by GCDCA. Cells not exposed/exposed to GCDCA were treated with Tolfenamic acid (TA) or Mithramycin A (MitA). (A) NOS-3 promoter activity ($n = 6$). (B) NOS-3 protein expression ($n = 3$). (C) NO-related end products ($n = 3$). (D) Caspase-3 activity ($n = 4$). Parameters were determined at 6 h (A, B, D) and 24 h (C) after treatment. Data expressed as mean ± SE. Statistically significant difference versus control group* or versus GCDCA group# are marked.

identified at positions −1386, −632 and −104 of the pNOS-3 (Table 1 and Fig. 1), and we used GAPDH and NOS-3 as positive controls of immunoprecipitation and gene expression, respectively (Fig. 8A). Immunoprecipitation of samples from HepG2 cells with anti-Sp1 antibody showed binding of Sp1 at positions −1386 ($p = 0.049$), −632 ($p = 0.034$) and −104 ($p = 0.034$) of the pNOS-3 after GCDCA administration (Fig. 8B). No binding of Sp1 to the pNOS-3 was detected at basal condition.

### 3.6. The in vivo model of cholestasis reproduces the GCDCA model in HepG2 cells

Biliary obstruction increased total and direct bilirubin, and hepatic injury markers GGT, AST and ALT in serum from rats as a consequence of cholestasis (Bile Duct Ligated group, BDL; $p < 0.001$) (Table 2). In the same way, the *in vivo* model of cholestasis was associated with: (A) macrophage invasion; (B)

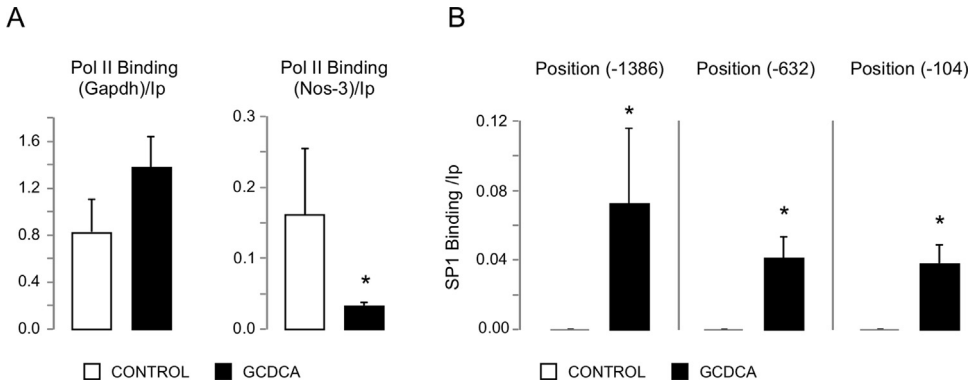


**Fig. 8.** Sp1 binding to the NOS-3 promoter. (A) Gene expression of glyceraldehyde 3-phosphate dehydrogenase (GAPDH) and NOS-3 as positive controls. (B) Enrichment of Sp1 binding to the NOS-3 promoter at positions −1386, −632 and −104. Data expressed as mean ± SE of three independents experiments. Statistically significant difference versus control group is marked*.

**Table 2**
Serum markers of liver function and cholestasis.

| | GGT (IU/l) | AST (IU/l) | ALT (IU/l) | TB (mg/dl) | DB (mg/dl) |
|---|---|---|---|---|---|
| SO group | 4 ± 0 | 62.92 ± 2.74 | 44 ± 6.65 | 0.13 ± 0.013 | 0.1 ± 0 |
| BDL group | 52.38 ± 6.90* | 332.54 ± 45.71* | 130.22 ± 17.85* | 9.13 ± 0.86* | 7.03 ± 0.66* |

SO, Sham operated group ($n = 13$); BDL, bile duct ligation group ($n = 13$). Data expressed as mean ± SE ($p \leq 0.05$). Statistically significant difference versus SO group is marked*.

the expression decrease of antioxidant genes Sod1 (34%), Sod2 (57%), catalase (25%), Gpx1 (23%) and Gpx4 (38%) ($p < 0.001$); (C) the increase of the ratio between the phosphorylated and non-phosphorylated forms of Sp1 (182%, $p = 0.024$); (D) the inhibition of Nos-3 mRNA expression (83%, $p = 0.001$) and (E) NOS-3 protein expression (83%, $p = 0.034$); and (F) the increase of caspase-3 activity (166%, $p = 0.033$) in liver tissue (Fig. 9).

Since the bile duct ligation induced the expression of the commonly used loading control proteins β-actin and GAPDH in the rat liver lysates (data not shown), we assessed the phosphorylated/non-phosphorylated protein ratio in the expression analysis of Sp1 in these samples (Fig. 9C). Similarly, the NOS-3 protein expression in the liver tissue was referred to the protein load (Fig. 9E).

## 4. Discussion

Although bile salts are not oxidants *per se*, these have been related to oxidative damage and NOS-3 expression deregulation [6], which are considered two main events in the pathogenesis of CLD. Actually, both, oxidative stress and NOS-3 expression regulation, are processes that are closely related and can be regulated to each other. Thus, using antioxidants or molecular treatments related to NO release or the recovery of NOS-3 expression has proven therapeutic efficacy against hepatotoxicity by bile acids. In the present study, we have investigated the relationship between these two biological processes and we have identified Sp1 as a candidate TF involved in the NOS-3 expression regulation during CLD.

In our cell model of cholestasis, GCDCA triggered hepatocellular damage and caused a reduction in NOS-3 expression by altering cellular redox homeostasis. The administration of the bile salt was related to the decrease of the combined activity of respiratory complexes II + III (but not of complexes I + III), which indicates a failure in the electron flow between respiratory complexes II and III. In this regard, the electron leak at the ubiquinone-complex III site is considered the main source of ROS generation during bile acid-induced toxicity [20] since it enhances the formation of $O_2^{\bullet -}$, which is a precursor of most other ROS [21]. The effect of GCDCA on the activity of mitochondrial complexes II + III was consistent with that associated with CDCA in isolated mitochondria from rat liver. However, in that approach, OXPHOS system was more sensitive to the non-conjugated form of the bile acid at lower concentrations.[22] As expected, oxidative stress prevention by administration of the cell permeable SOD mimetic MnTBAP was associated with the gene expression recovery of the cellular antioxidant system and the increase of the NOS-3 expression and activity. This resulted in an increase in cell survival as measured by the decrease on caspase-3 activity and LDH release. Concerning the use of MnTBAP as a specific superoxide scavenger, it should be noted that non-porphyrin Mn species that appears as impurities in commercial MnTBAP preparations exhibit SOD-like activity and are very effective in dismuting $O_2^{\bullet -}$ [23,24]. Furthermore, the administration of ubiquinone through the mitochondria-targeted antioxidant MitoQ also recovered the activity of the pNOS-3. According to the literature, MitoQ caused the activity recovery of the respiratory complex II + III [14] in the presence of GCDCA. This was related to oxidative stress reduction, NOS-3 protein increase and cellular protection against GCDCA [9]. NOS-2 gene expression was not detected before or after GCDCA treatment (data not shown).

Functional characteristics of the human pNOS-3 are extremely complex, and particularly interrelation among cis-elements remains to be elucidated. Different conditions involved in the generation of oxidative stress may up-regulate [25] or down-regulate [26] the pNOS-3. However, there is no evidence about the elements involved in the regulation of NOS-3 expression during GCDCA-induced cytotoxicity. Bioinformatic analysis of the pNOS-3 sequence identified different TFBS for Sp1. This was particularly interesting because Sp1 is a redox-sensitive TF involved in a variety of cellular processes including the NOS-3 expression regulation [27–29] and the bile acid-induced cell apoptosis [30]. The cellular response to GCDCA was characterised by the increase of expression and activation of Sp1 (which was associated with the activation of MAPKs JNK and ERK1/2) and by a greater binding capacity of this to the TFBS identified in the pNOS-3 at positions −1386, −632 and −104. This resulted in a decrease of pNOS-3 activity and NOS-3 protein expression. The administration of MnTBAP significantly reduced the GCDCA-dependent activation of Sp1, and caused the recovery of the pNOS-3 transcriptional activity and NOS-3 expression, the accumulation of NO end-products nitrates and nitrites, and the reduction of cell death related parameters. Similarly, MitoQ reduced the expression and/or activation of Sp1 and induced the pNOS-3 activity, which was related to the NOS-3 expression/activity increase and the cell survival [9]. This is consistent with a model of gene expression regulation by oxidative stress instead of direct interaction with TFs [31], and agrees with the MAPKs regulation mechanism through oxidative stress induced by bile acids [32].

Sp1 binding to the pNOS-3 has been related to NOS-3 up-regulation induced by cytotoxicity [33] or by free radical scavenging [34]. Kumar et al. demonstrated that Sp1 binding to the pNOS-3 regulates the promoter activity in response to oxidative stress [26]. However, in that report, the addition of $H_2O_2$ decreased the promoter activity by reducing the binding capability of Sp1. Here, we also observed a promoter activity decrease as a consequence of a higher intracellular production of ROS, but it was associated with an increase of Sp1 binding to the pNOS-3. The specific inhibition of Sp1 with TA (which induces the degradation of Sp1, Sp3 and Sp4) [35] or MitA (which selectively displace Sp1 from its binding site) [36,37] resulted in cellular protection against GCDCA-induced cell death through the same mechanism described above for the antioxidants. Thus, Sp1 inhibition caused the recovery of the pNOS-3 activity and the NOS-3 expression in GCDCA-treated HepG2 cells. These results suggest that Sp1 is not essential for NOS-3 expression. Actually, Sp1 could function as a transcriptional repressor of NOS-3 gene expression through direct binding to the promoter sequence at positions described above. In this regard, it should be noted that histone deacetylase 1 (HDAC1) plays a critical role in the NOS-3 repression [38] through its direct binding to Sp1 [39]. Interestingly, the pNOS-3 activity can be also regulated by methylation [40], which is a process that is associated with histone deacetylation [41].

In the model of experimental cholestasis *in vivo*, the reduction of the cellular antioxidant status (which reflects a liver response to

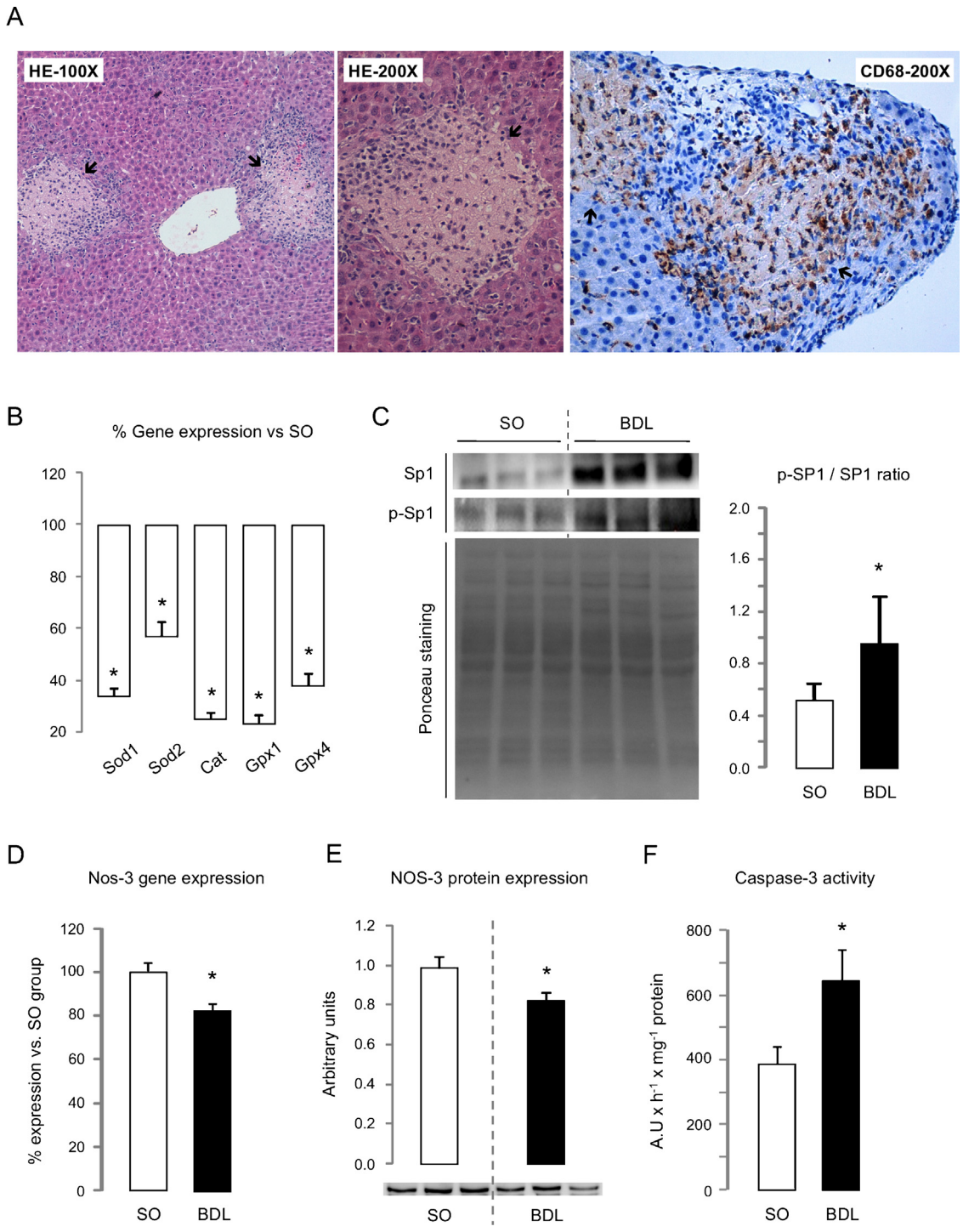


**Fig. 9.** Animal model of cholestasis. (A) CD68 expression was analysed by immunohistochemistry in order to confirm the presence or absence of macrophage invasion previously evaluated by HE staining. The macrophage invasion foci are marked with arrows. The number of positive cases in SO group ($n = 13$) and BDL group ($n = 13$) were 1 and 10, respectively. (B) Expression levels of antioxidant genes Sod1, Sod2, catalase, Gpx1 and Gpx4. (C) Representative images for Ponceau staining and western blots for (p-)Sp1. The densitometry analysis of blots is showed as the ratio p-Sp1/Sp1. (D) NOS-3 mRNA expression. (E) Representative western blot for NOS-3 expression (SO group, $n = 10$; BDL group, $n = 10$). (F) Caspase-3 activity. Data expressed as mean ± SE. Representative Western blot images include three independent samples from each group. Statistically significant difference versus SO group is marked*.

oxidative stress) was related to the activation of Sp1, the inhibition of NOS-3 expression and the hepatocellular damage. Bile duct ligation induced the expression of proteins β-actin and GAPDH. This result is not surprising since the hepatic cholestasis was associated with tissue fibrosis [15], and liver fibrosis has been previously linked to changes in the expression of commonly used loading control proteins [42,43]. We have previously shown that NOS-2 overexpression in the BDL group is associated with the hepatocellular injury [15]. According to the results of the present study, the adverse effects exerted by NO during cholestatic injury might be due to both the increase in NOS-2 and the reduction in NOS-3 expression. This agrees with the reported during the

progression of liver fibrosis [44]. Here, we found evidences for macrophage invasion in liver tissue sections from BDL animals. This observation was interesting because activated macrophages are an important source of ROS [45] and NOS-2-derived NO [46], and have been associated with many inflammatory models of liver injury. Thus, it is generally accepted that innate immune cells including Kupffer cells and infiltrating macrophages are activated after liver damage and can deteriorate the initial liver injury [47]. Because of this, we cannot rule out a significant role for macrophage invasion in the NOS-3 expression regulation by oxidative stress during cholestasis, or in the change of NOS-2/NOS-3 expression ratio during the progression of chronic liver injury.

In summary, GCDCA-induced oxidative stress was related to: (1) the expression and activation increase of Sp1, (2) the increased binding of Sp1 to the pNOS-3 at described positions, (3) the decrease of the NOS-3 promoter activity and the NOS-3 protein expression and associated activity, and (4) the cell death. In the cellular model of cholestasis, the inhibition of Sp1 was related to cell survival. Further investigation is required to determine the therapeutic value of Sp1 inhibitors for the treatment of cholestatic liver diseases. In this regard, it is important to note that TA is a non-steroidal anti-inflammatory drug (NSAID) whose side effects include dose-related gastrointestinal toxicity [48] and drug-induced liver injury [49]. On the other hand, the antibiotic MitA causes undesirable toxic side effects at doses commonly used to treat different diseases [50,51]. Therefore, care should be taken when assessing the therapeutic power of these drugs. The regulation of Sp1 by oxidative stress and the involvement of NOS-3 in this process represent a new mechanism by which the accumulation of bile acids causes a cytotoxic effect, and provides a new potential therapeutic target for CLD.

## Funding

This work was supported by the Instituto de Salud Carlos III (grant number PI05/0703). G. Ferrín was supported by the Biomedical Research Centre Network Digestive and Liver Diseases (CIBEREHD).

## Acknowledgment

We thank the Dr. Huige Li from the Department of Pharmacology of Johannes Gutenberg University (Mainz, Germany) for providing us with the NOS-3 promoter sequence.

## References

[1] M.E. Guicciardi, G.J. Gores, Cholestatic hepatocellular injury: what do we know and how should we proceed, J. Hepatol. 42 (2005) 297–300.
[2] M.M. Tiao, T.K. Lin, C.W. Liou, P.W. Wang, J.B. Chen, F.Y. Kuo, et al., Early transcriptional deregulation of hepatic mitochondrial biogenesis and its consequent effects on murine cholestatic liver injury, Apoptosis 14 (2009) 890–899.
[3] B. Yerushalmi, R. Dahl, M.W. Devereaux, E. Gumpricht, R.J. Sokol, Bile acid-induced rat hepatocyte apoptosis is inhibited by antioxidants and blockers of the mitochondrial permeability transition, Hepatology 33 (2001) 616–626.
[4] M.G. Clemens, Nitric oxide in liver injury, Hepatology 30 (1999) 1–5.
[5] D. Rockey, The cellular pathogenesis of portal hypertension: stellate cell contractility, endothelin, and nitric oxide, Hepatology 25 (1997) 2–5.
[6] E. Biecker, J. Trebicka, A. Kang, M. Hennenberg, T. Sauerbruch, J. Heller, Treatment of bile duct-ligated rats with the nitric oxide synthase transcription enhancer AVE 9488 ameliorates portal hypertension, Liver Int. 28 (2008) 331–338.
[7] K.C. Lee, Y.Y. Yang, Y.T. Huang, F.Y. Lee, M.C. Hou, H.C. Lin, et al., Administration of a low dose of sildenafil for 1 week decreases intrahepatic resistance in rats with biliary cirrhosis: the role of NO bioavailability, Clin. Sci. (Lond.) 119 (2010) 45–55.
[8] S. Gonzalez-Rubio, C.I. Linares, R.I. Bello, R. Gonzalez, G. Ferrin, A.B. Hidalgo, et al., Calcium-dependent nitric oxide production is involved in the cytoprotective properties of n-acetylcysteine in glycochenodeoxycholic acid-induced cell death in hepatocytes, Toxicol. Appl. Pharmacol. 242 (2010) 165–172.
[9] S. Gonzalez-Rubio, A.B. Hidalgo, G. Ferrin, R.I. Bello, R. Gonzalez, M.D. Gahete, et al., Mitochondrial-driven ubiquinone enhances extracellular calcium-dependent nitric oxide production and reduces glycochenodeoxycholic acid-induced cell death in hepatocytes, Chem. Res. Toxicol. 22 (2009) 1984–1991.
[10] R. Gonzalez, A. Cruz, G. Ferrin, P. Lopez-Cillero, R. Fernandez-Rodriguez, J. Briceno, et al., Nitric oxide mimics transcriptional and post-translational regulation during alpha-tocopherol cytoprotection against glycochenodeoxycholate-induced cell death in hepatocytes, J. Hepatol. 55 (2011) 133–144.
[11] D.A. Wink, K.M. Miranda, M.G. Espey, R.M. Pluta, S.J. Hewett, C. Colton, et al., Mechanisms of the antioxidant effects of nitric oxide, Antioxid. Redox Signal. 3 (2001) 203–213.
[12] M. Kelm, Nitric oxide metabolism and breakdown, Biochim. Biophys. Acta 1411 (1999) 273–289.
[13] H.T. Chung, H.O. Pae, B.M. Choi, T.R. Billiar, Y.M. Kim, Nitric oxide as a bioregulator of apoptosis, Biochem. Biophys. Res. Commun. 282 (2001) 1075–1079.
[14] G.F. Kelso, C.M. Porteous, C.V. Coulter, G. Hughes, W.K. Porteous, E.C. Ledgerwood, et al., Selective targeting of a redox-active ubiquinone to mitochondria within cells: antioxidant and antiapoptotic properties, J. Biol. Chem. 276 (2001) 4588–4596.
[15] L.M. Lopez-Sanchez, F.J. Corrales, M. Barcos, I. Espejo, J.R. Munoz-Castaneda, A. Rodriguez-Ariza, Inhibition of nitric oxide synthesis during induced cholestasis ameliorates hepatocellular injury by facilitating S-nitrosothiol homeostasis, Lab. Invest. 90 (2010) 116–127.
[16] A. Wojtala, M. Bonora, D. Malinska, P. Pinton, J. Duszynski, M.R. Wieckowski, Methods to monitor ROS production by fluorescence microscopy and fluorometry, Methods Enzymol. 542 (2014) 243–262.
[17] E. Fernandez-Vizarra, M.J. Lopez-Perez, J.A. Enriquez, Isolation of biogenetically competent mitochondria from mammalian tissues and cultured cells, Methods 26 (2002) 292–297.
[18] E. Lapuente-Brun, R. Moreno-Loshuertos, R. Acin-Perez, A. Latorre-Pellicer, C. Colas, E. Balsa, et al., Supercomplex assembly determines electron flux in the mitochondrial electron transport chain, Science 340 (2013) 1567–1570.
[19] A. Fernandez-Alvarez, M. Soledad Alvarez, C. Cucarella, M. Casado, Characterization of the human insulin-induced gene 2 (INSIG2) promoter: the role of Ets-binding motifs, J. Biol. Chem. 285 (2010) 11765–11774.
[20] H. Higuchi, G.J. Gores, Bile acid-mediates apoptosis in cholestasis, in: M. Trauner, P.L.M. Jansen (Eds.), Molecular Pathogenesis of Cholestasis, Eurekah.com/Landes Bioscience, NY, USA, 2004, pp. 126–134.
[21] J.F. Turrens, Mitochondrial formation of reactive oxygen species, J. Physiol. 552 (2003) 335–344.
[22] S. Krahenbuhl, C. Talos, S. Fischer, J. Reichen, Toxicity of bile acids on the electron transport chain of isolated rat liver mitochondria, Hepatology 19 (1994) 471–479.
[23] D.C. da Silva, G. DeFreitas-Silva, E. do Nascimento, J.S. Reboucas, P.J. Barbeira, M.E. de Carvalho, et al., Spectral, electrochemical, and catalytic properties of a homologous series of manganese porphyrins as cytochrome P450 model: the effect of the degree of beta-bromination, J. Inorg. Biochem. 102 (2008) 1932–1941.
[24] I. Batinic-Haberle, S. Cuzzocrea, J.S. Reboucas, G. Ferrer-Sueta, E. Mazzon, R. Di Paola, et al., Pure MnTBAP selectively scavenges peroxynitrite over superoxide: comparison of pure and commercial MnTBAP samples to MnTE-2-PyP in two models of oxidative stress injury, an SOD-specific Escherichia coli model and carrageenan-induced pleurisy, Free Radic. Biol. Med. 46 (2009) 192–201.
[25] J. Min, Y.M. Jin, J.S. Moon, M.S. Sung, S.A. Jo, I. Jo, Hypoxia-induced endothelial NO synthase gene transcriptional activation is mediated through the tax-responsive element in endothelial cells, Hypertension 47 (2006) 1189–1196.
[26] S. Kumar, X. Sun, D.A. Wiseman, J. Tian, N.S. Umapathy, A.D. Verin, et al., Hydrogen peroxide decreases endothelial nitric oxide synthase promoter activity through the inhibition of Sp1 activity, DNA Cell. Biol. 28 (2009) 119–129.
[27] P.A. Marsden, H.H. Heng, S.W. Scherer, R.J. Stewart, A.V. Hall, X.M. Shi, et al., Structure and chromosomal localization of the human constitutive endothelial nitric oxide synthase gene, J. Biol. Chem. 268 (1993) 17478–17488.
[28] F. Xing, Y. Jiang, J. Liu, K. Zhao, Y. Mo, Q. Qin, et al., Role of AP1 element in the activation of human eNOS promoter by lysophosphatidylcholine, J. Cell Biochem. 98 (2006) 872–884.
[29] S. Wariishi, K. Miyahara, K. Toda, S. Ogoshi, Y. Doi, S. Ohnishi, et al., A SP1 binding site in the GC-rich region is essential for a core promoter activity of the human endothelial nitric oxide synthase gene, Biochem. Biophys. Res. Commun. 216 (1995) 729–735.
[30] H. Higuchi, A. Grambihler, A. Canbay, S.F. Bronk, G.J. Gores, Bile acids up-regulate death receptor 5/TRAIL-receptor 2 expression via a c-Jun N-terminal kinase-dependent pathway involving Sp1, J. Biol. Chem. 279 (2004) 51–60.
[31] H.M. Tse, M.J. Milton, J.D. Piganelli, Mechanistic analysis of the immunomodulatory effects of a catalytic antioxidant on antigen-presenting cells: implication for their use in targeting oxidation-reduction reactions in innate immunity, Free Radic. Biol. Med. 36 (2004) 233–247.
[32] Y. Fang, S.I. Han, C. Mitchell, S. Gupta, E. Studer, S. Grant, et al., Bile acids induce mitochondrial ROS, which promote activation of receptor tyrosine kinases and signaling pathways in rat hepatocytes, Hepatology 40 (2004) 961–971.
[33] K. Cieslik, A. Zembowicz, J.L. Tang, K.K. Wu, Transcriptional regulation of endothelial nitric-oxide synthase by lysophosphatidylcholine, J. Biol. Chem. 273 (1998) 14885–14890.
[34] J.W. Xu, K. Ikeda, Y. Yamori, Upregulation of endothelial nitric oxide synthase by cyanidin-3-glucoside, a typical anthocyanin pigment, Hypertension 44 (2004) 217–222.
[35] M. Abdelrahim, C.H. Baker, J.L. Abbruzzese, S. Safe, Tolfenamic acid and pancreatic cancer growth, angiogenesis, and Sp protein degradation, J. Natl. Cancer Inst. 98 (2006) 855–868.
[36] R.C. Snyder, R. Ray, S. Blume, D.M. Miller, Mithramycin blocks transcriptional initiation of the c-myc P1 and P2 promoters, Biochemistry 30 (1991) 4290–4297.

[37] S.W. Blume, R.C. Snyder, R. Ray, S. Thomas, C.A. Koller, D.M. Miller, Mithramycin inhibits SP1 binding and selectively inhibits transcriptional activity of the dihydrofolate reductase gene in vitro and in vivo, J. Clin. Invest. 88 (1991) 1613–1621.
[38] Y. Gan, Y.H. Shen, J. Wang, X. Wang, B. Utama, X.L. Wang, Role of histone deacetylation in cell-specific expression of endothelial nitric-oxide synthase, J. Biol. Chem. 280 (2005) 16467–16475.
[39] A. Doetzlhofer, H. Rotheneder, G. Lagger, M. Koranda, V. Kurtev, G. Brosch, et al., Histone deacetylase 1 can repress transcription by binding to Sp1, Mol. Cell Biol. 19 (1999) 5504–5511.
[40] Y. Chan, J.E. Fish, C. D'Abreo, S. Lin, G.B. Robb, A.M. Teichert, et al., The cell-specific expression of endothelial nitric-oxide synthase: a role for DNA methylation, J. Biol. Chem. 279 (2004) 35087–35100.
[41] P.L. Jones, G.J. Veenstra, P.A. Wade, D. Vermaak, S.U. Kass, N. Landsberger, et al., Methylated DNA and MeCP2 recruit histone deacetylase to repress transcription, Nat. Genet. 19 (1998) 187–191.
[42] M. Congiu, J.L. Slavin, P.V. Desmond, Expression of common housekeeping genes is affected by disease in human hepatitis C virus-infected liver, Liver Int. 31 (2011) 386–390.
[43] H. Boujedidi, L. Bouchet-Delbos, A.M. Cassard-Doulcier, M. Njike-Nakseu, S. Maitre, S. Prevot, et al., Housekeeping gene variability in the liver of alcoholic patients, Alcohol Clin. Exp. Res. 36 (2012) 258–266.
[44] T.M. Leung, G.L. Tipoe, E.C. Liong, T.Y. Lau, M.L. Fung, A.A. Nanji, Endothelial nitric oxide synthase is a critical factor in experimental liver fibrosis, Int. J. Exp. Pathol. 89 (2008) 241–250.
[45] H. Jaeschke, Reactive oxygen and mechanisms of inflammatory liver injury: present concepts, J. Gastroenterol. Hepatol. 26 (Suppl. 1) (2011) 173–179.
[46] C.J. Lowenstein, E. Padalko, iNOS (NOS2) at a glance, J. Cell Sci. 117 (2004) 2865–2867.
[47] H. Jaeschke, Mechanisms of liver injury. II. Mechanisms of neutrophil-induced liver cell injury during hepatic ischemia-reperfusion and other acute inflammatory conditions, Am. J. Physiol. Gastrointest. Liver Physiol. 290 (2006) G1083–G1088.
[48] D. Bjorkman, Nonsteroidal anti-inflammatory drug-associated toxicity of the liver, lower gastrointestinal tract, and esophagus, Am. J. Med. 105 (1998) 17S–21S.
[49] M.D. Leise, J.J. Poterucha, J.A. Talwalkar, Drug-induced liver injury, Mayo Clin. Proc. 89 (2014) 95–106.
[50] L. Green, R.C. Donehower, Hepatic toxicity of low doses of mithramycin in hypercalcemia, Cancer Treat. Rep. 68 (1984) 1379–1381.
[51] L.E. Nunez, S.E. Nybo, J. Gonzalez-Sabin, M. Perez, N. Menendez, A.F. Brana, et al., A novel mithramycin analogue with high antitumor activity and less toxicity generated by combinatorial biosynthesis, J. Med. Chem. 55 (2012) 5813–5825.